Journal of Organometallic Chemistry 880 (2019) 91–97

Contents lists available at ScienceDirect

Journal of Organometallic Chemistry

journal homepage: www.elsevier.com/locate/jorganchem

Naphthyl C8-H hydrogen activation and synthesis of organometallic ruthenium complex: Crystal structure of hydride intermediates and catalytic transfer hydrogenation

Manju Bala*, Anand Ratnam, Rajan Kumar, Kaushik Ghosh**

Department of Chemistry, Indian Institute of Technology, Roorkee, Roorkee, 247667, Uttarakhand, India

ARTICLE INFO

Article history:
Received 4 July 2018
Received in revised form
16 October 2018
Accepted 31 October 2018
Available online 3 November 2018

Keywords:
Ruthenium(II) organometallics
Naphthyl C8-H activation
Hydride
Catalytic transfer hydrogenation

ABSTRACT

Organometallic ruthenium(II) complex [Ru(L^1C^N^N)(PPh_3)$_2$(CO)] (**1**) [where L^1H_2 is (E)–N-((1H-pyrrol-2-yl)methylene)naphthalen-1-amine] [H represents dissociable proton] was synthesized via C–H bond activation using different synthetic strategies. Ruthenium hydrido carbonyl complexes [Ru(L^1N^N)(PPh_3)$_2$(CO)H] (**2**) [where L^1H_2 is (E)–N-((1H-pyrrol-2-yl)methylene)naphthalen-1-amine] and [Ru(L^2N^N)(PPh_3)$_2$(CO)H] (**3**) [where L^2H_2 is (E)–N-((1H-pyrrol-2-yl)methylene)-1-phenylmethanamine] were isolated. All the complexes were characterized by UV–Vis, IR and NMR spectral studies. Molecular structures of complexes **1**, **2** and **3** were authenticated using X-ray crystallography. Geometry optimisation of the complexes **1**–**3** have been performed using Density Functional Theory (DFT) studies. Time-dependent DFT calculations were performed to better understand the electronic properties of complexes **1**–**3**. Complex **1** was utilized as catalyst in transfer hydrogenation of ketones. On the basis of literature study, the plausible mechanisms were proposed for hydride formation and catalytic transfer hydrogenation.

1. Introduction

Cyclometalation, one of the most convenient methods for synthesis of organometallic entities, has gained significant current interest probably because of mildest route followed for activation of strong C–H bonds [1]. The chemistry of organometallic compounds has become fast grown area in the field of chemical research because of vast applications of these complexes in catalysis, organic transformation, bioorganometallic chemistry, photophysical devices etc. [1] Our recent reports [2] on ruthenium organometallics clearly indicated the necessity of at least one hard donor present in the bidentate ligand frame to synthesize cyclometalated ruthenium complexes, but none of the report describes the naphthyl C8-H bond activation. However, only few reports are available in literature on naphthyl C–H activation using ruthenium complexes [3–7] and it still remains the challenging area of chemical research.

It is well known that hydrides are reactive intermediates or catalysts in various chemical reactions [8]. Both, the laboratory and industrial applications of transition metal hydrides including hydrogenation, catalytic and stoichiometric transformations, olefin isomerization and hydroformylation reactions, electrochemical H_2 evolution, reduction of CO_2 to carbon-based fuels, have made their chemistry an important area of research [9]. These prompted us to investigate the chemistry of ruthenium hydride complexes.

From literature study, it was found that deprotonated pyrrole nitrogen is a hard donor and stabilizes metal in higher oxidation state [10,11]. This encouraged us to synthesize ligands L^1H_2 and L^2H_2 (shown in Scheme 1).

In the present report, we describe the syntheses and spectral characterization of organometallic ruthenium(II) complex [Ru(L^1C^N^N)(PPh_3)$_2$(CO)] (**1**) (shown in Scheme 2) and ruthenium hydrido carbonyl complexes [Ru(L^1N^N)(PPh_3)$_2$(CO)H] (**2**) [where L^1H_2 is (E)–N-((1H-pyrrol-2-yl)methylene)naphthalen-1-amine] and [Ru(L^2N^N)(PPh_3)$_2$(CO)H] (**3**) [where L^2H_2 is (E)–N-((1H-pyrrol-2-yl)methylene)-1-phenylmethanamine] [H represents dissociable proton] (shown in Scheme 2). Complex **1** was utilized for

* Corresponding author.
** Corresponding author.
E-mail address: manjudcy@gmail.com (M. Bala).

https://doi.org/10.1016/j.jorganchem.2018.10.034
0022-328X/

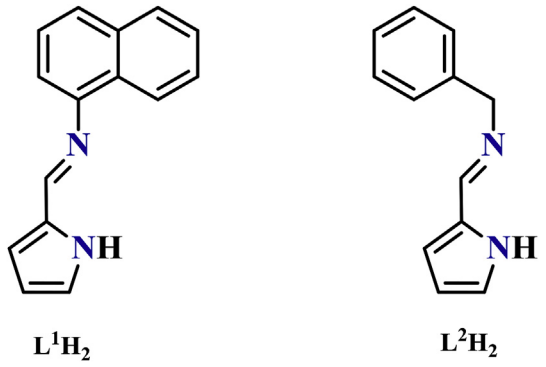

L^1H_2 L^2H_2

Scheme 1. Ligands L^1H_2 and L^2H_2.

transfer hydrogenation of ketones. Geometries of **1**, **2** and **3** were authenticated using X-ray crystallography.

2. Experimental section

2.1. Materials and methods

All the reagents naphthalene-1-amine, phenylmethanamine, pyrrole-2-carbaldehyde, (Himedia Laboratories Pvt. Ltd., Mumbai, India) were of analytical grade. $RuCl_3.3H_2O$ was purchased from Loba Chemie Pvt. Ltd., Mumbai, India. Triphenylphosphine (SRL, Mumbai, India) was used as obtained. The precursor $[Ru(PPh_3)_3Cl_2]$ was synthesized using the procedure reported earlier [12]. Infrared spectra were recorded with Thermo Nicolet Nexus FT–IR spectrometer, as KBr pellets using 16 scans and were reported in cm^{-1}. ^1H NMR spectra of all complexes in the deuterated solvents were recorded on JEOL, 400 MHz spectrometer. Electronic absorption spectra of all complexes in dichloromethane solvent were recorded with an Evolution 600, Thermo Scientific (Shimadzu) UV–vis spectrophotometer.

2.2. Syntheses of ligands

N-((1H-pyrrol-2-yl)methylene)naphthalen-1-amine (L^1H_2): A solution of pyrrole-2-carbaldehyde (3 mmol) in 5 mL methanol was added dropwise to solution of naphthalene-1-amine (3 mmol) in 10 mL methanol with stirring. After 1 day of continous stirring the brown coloured precipitate was filtered and washed with small amount of methanol. Yield: (70%). UV–vis (CH_2Cl_2; λ_{max}, nm (ε, $M^{-1}\,cm^{-1}$)): 241 (69,900), 341 (47,600). ^1H NMR (chloroform-d, 400 MHz): δ 10.11 (s, 1H), 8.36–6.28 (11H).

N-((1H-pyrrol-2-yl)methylene)-1-phenylmethanamine (L^2H_2): Ligand L^2H_2 was synthesized from the reaction of pyrrole-2-carbaldehyde with phenylmethanamine in the same way as for ligand L^1H_2. Yield: (75%). UV–vis (CH_2Cl_2; λ_{max}, nm (ε, $M^{-1}\,cm^{-1}$)): 282 (1,47000), 330 (22494). ^1H NMR (DMSO-d_6, 400 MHz): δ 11.41 (s, 1H), 8.17 (s, 1H), 7.27–6.07 (8H), 4.62 (s, 2H).

2.3. Syntheses of metal complexes

Synthesis of [Ru(L^1C^N^N)(PPh_3)$_2$(CO)] (1): Complex **1** was synthesized in two ways: (i) A batch of $Ru(PPh_3)_3Cl_2$ (0.1 mmol) was added directly to a solution of ligand L^1H_2 (0.15 mmol) in 2-methoxy ethanol and colour of solution was transformed to reddish after 10 min. This reddish solution was refluxed for 1 h and orange coloured solid was precipitated out, which was filtered and washed with small amount of methanol. Yield: 60% (ii) Complex [Ru(L^1C^N^N)(PPh_3)$_2$(CO)] (**1**) was also synthesized from the complex **2** by refluxing in 2-methoxy ethanol for 10 min. IR (KBr disk, in cm^{-1}): 1913(ν_{CO}), 1588 ($\nu_{C=N}$), 753, 692, 520 (ν_{PPh3}) cm^{-1}. UV–vis (CH_2Cl_2; λ_{max}, nm (ε, $M^{-1}\,cm^{-1}$)): 275 (40,000), 405 (23,330), 485 (20,000), 517 (16,660). ^1H NMR (chloroform-d, 400 MHz): δ 7.601–7.347 (m, 8H), 7.215–7.081 (m, 27H), 6.804 (t, 1H), 6.735 (d, 1H), 6.541 (d, 1H), 6.441 (d, 1H), 6.081 (m, 2H).

Synthesis of [Ru(L^1N^N)(PPh_3)$_2$(CO)H] (2): To a solution of ligand L^1H_2 (0.15 mmol) and triethylamine in methanol, a batch of $Ru(PPh_3)_3Cl_2$ (0.1 mmol) was added and colour of solution was changed to light reddish brown. This reddish brown solution was refluxed for 4 h and yellowish brown coloured solid was precipitated out, filtered and washed with small amount of methanol. Yield: (65%). IR (KBr disk, in cm^{-1}): 1924(ν_{CO}), 1555 ($\nu_{C=N}$), 744, 691, 516 (ν_{PPh3}) cm^{-1}. UV–vis (CH_2Cl_2; λ_{max}, nm (ε, $M^{-1}\,cm^{-1}$)): 239 (13812), 397 (3500). ^1H NMR (chloroform-d, 400 MHz): δ −11.72 (t, 1H), 7.601–7.347 (m, 8H), 7.215–7.081 (m, 27H), 6.804 (t, 1H), 6.735 (d, 1H), 6.541 (d, 1H), 6.441 (d, 1H), 6.081 (m, 2H).

Synthesis of [Ru(L^2N^N)(PPh_3)$_2$(CO)H] (3): Complex [Ru(L^2N^N)(PPh_3)$_2$(CO)H] (**3**) was synthesized by following the same procedure as for **2** from the reaction of $Ru(PPh_3)_3Cl_2$ with ligand L^2H_2. Yield: 70%. IR (KBr disk, in cm^{-1}): 1910(ν_{CO}), 1587 ($\nu_{C=N}$), 745, 695, 520(ν_{PPh3}) cm^{-1}. UV–vis (CH_2Cl_2; λ_{max}, nm (ε, $M^{-1}\,cm^{-1}$)): 230 (100,000), 338 (34,659).

X–ray crystallography: Single crystal of complexes **1**, **2** and **3** were obtained via layering of hexane over a solution of dichloromethane which were suitable for diffraction study. The X–ray data collection and processing of complexes **1**, **2** and **3** were carried out using Bruker Kappa Apex–II CCD diffractometer and graphite monochromated Mo–Kα radiation ($\lambda = 0.71073$ Å) at 273 K. Structure solutions, refinement and data output were carried out with

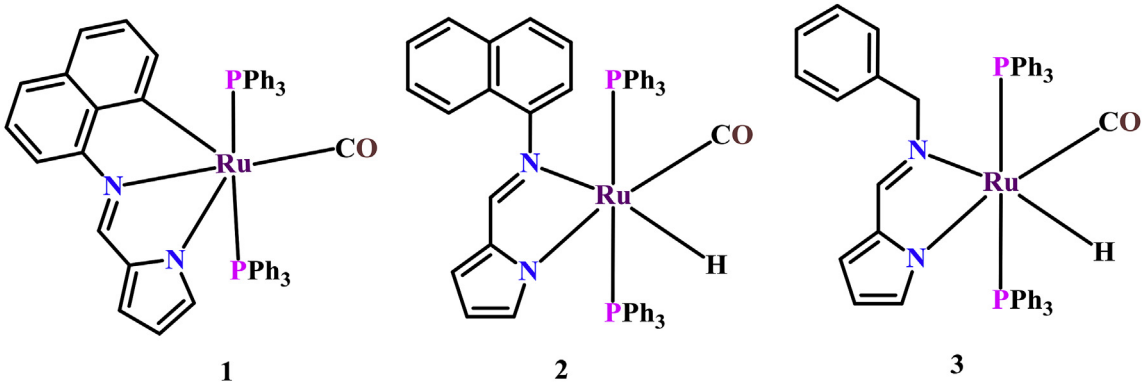

1 2 3

Scheme 2. Complexes **1**, **2** and **3**.

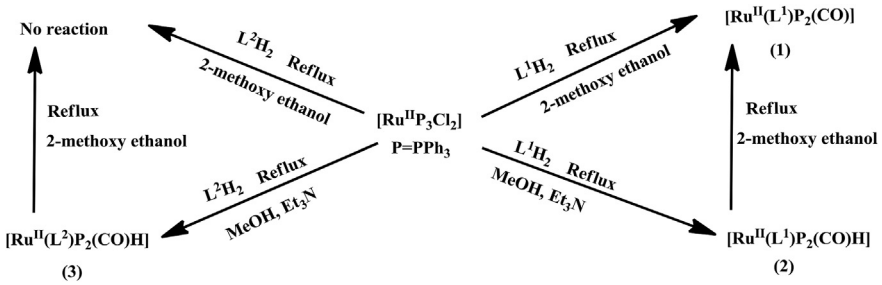

Scheme 3. Synthetic routes of complexes **1**, **2**, and **3**.

the SHELXTL program [13,14]. All non–hydrogen atoms were refined anisotropically and hydrogen atoms were placed in geometrically calculated positions and refined using a riding model. Images were produced with the DIAMOND program [15].

2.4. DFT study and computational details

The DFT calculations for complexes **1**, **2** and **3** were carried out using Gaussian 09 program package.[16,17] The Becke's three parameters hybrid exchange functional with the Lee–Yang–Parr (LYP) nonlocal correlation functional was used throughout the computational study [16,17]. A LANL2DZ basis set for ruthenium metal was used in the calculation. Coordinates from single crystal X-ray structures of all the complexes were used as input data for the optimisation of geometries. Pictorial representations of frontier molecular orbitals were created using the Gauss View-5 program. To evaluate the electronic transitions, time dependent density functional theory (TD-DFT) calculations were also performed on the optimised geometries.

2.5. Synthetic procedure for catalytic transfer hydrogenation

In a microwave reaction vial with a closed cap, a mixture containing ketone (1 mmol), the catalyst (known mol percent) and base (known mol percent) in 5 mL of isopropanol was heated on the oil bath with continous stirring at 85 °C for suitable period of time as mentioned. After the usual workup (reported in literature), the reaction product dissolved in hexane was analyzed by GC-MS.

3. Results and discussion

3.1. Syntheses

Ligands L^1H_2 and L^2H_2 were obtained by condensation reaction of pyrrole-2-carbaldehyde with naphthalene-1-amine and phenylmethanamine, respectively, in 20 mL methanol with continuous stirring. Complex [Ru(L^1C^N^N)(PPh_3)$_2$(CO)] (**1**) was synthesized in two different ways (shown in Scheme 3). The complexes [Ru(L^1N^N)(PPh_3)$_2$(CO)H] (**2**) and [Ru(L^2N^N)(PPh_3)$_2$(CO)H] (**3**) were synthesized (shown in Scheme 3) by the reaction of Ru(PPh_3)$_3$$Cl_2$ in methanol and triethylamine with the Schiff base ligands L^1H_2 and L^2H_2 (shown in Scheme 1), respectively. Plausible mechanism for the syntheses of complexes **1** and **2** (shown in Scheme 4) is in accordance with reported literature [5a,18]. Complex **3** was formed in a similar way as for complex **2**. All the complexes were soluble in dichloromethane and dimethylsulfoxide.

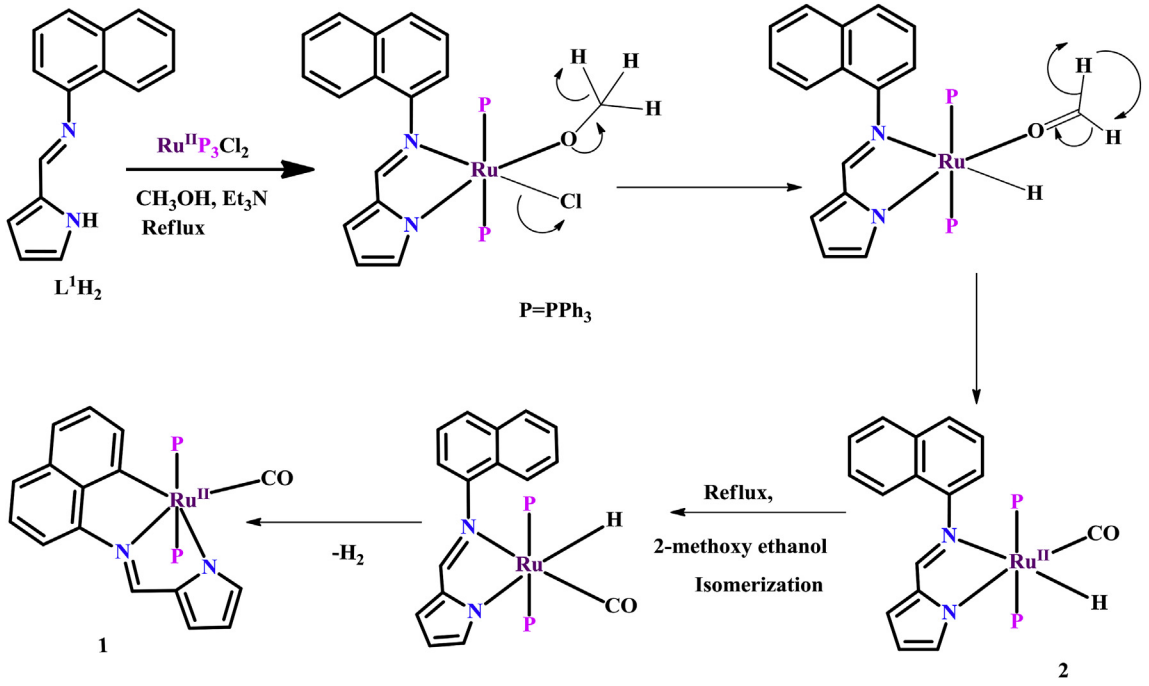

Scheme 4. Plausible mechanism for the syntheses of complexes **2** and **1**.

3.2. Spectroscopic studies

In the IR spectra of complexes **1**–**3**, the C–O stretching frequency (ν_{CO}) was observed around 1910–1920 cm^{-1} [5,18]. In all the complexes **1**–**3**, the peaks in the range 745–750 cm^{-1}, 690–695 cm^{-1} and 514–520 cm^{-1} confirmed the presence of axial PPh_3 ligands [5a,18] (shown in Figs. S1, S2 and S3 respectively).

The electronic absorption spectra of complexes **1**–**3** were displayed in Figs. S4, S5 and S6 respectively. In complex **1**, band near 275 nm probably due to ligand centred charge transfer transition was observed and bands at 405 nm, 485 nm, 517 nm were recognized to be metal to ligand charge transfer (MLCT) transition. In complex **2**, we observed a band with λ_{max} near 239 nm probably due to ligand centred charge transfer transition and a band with λ_{max} near 397 nm which was probably due to metal to ligand charge transfer (MLCT) transition. In complex **3**, a band with λ_{max} near 338 nm was recognized to be metal to ligand charge transfer (MLCT) transition.

In the ligands (L^1H_2) and (L^2H_2), we observed peaks near 10.11 ppm and 11.41 ppm respectively, which were due to the presence of pyrrole (–NH–) proton (Figs. S7 and S8). All the complexes were confirmed to be diamagnetic by ^1H NMR spectral studies. The ^1H NMR spectra of **1** and **2** were displayed in Figs. S9 and S10 respectively.

3.3. Depiction of molecular structure

The crystal structures of the complexes [Ru(L^1C^N^N)(PPh_3)$_2$(CO)] (**1**), [Ru(L^1N^N)(PPh_3)$_2$(CO)H] (**2**) and [Ru(L^2N^N)(PPh_3)$_2$(CO)H] (**3**) and are depicted in Figs. 1–3 respectively.

The selected bond lengths and bond angles of complexes **1**–**3** along with theoretical values are given in Table 1. Crystal data collection and refinement detail of the structures of complexes **1**–**3** are summarized in Table S1. In the crystal structure of **1**, the equatorial plane consisted of N(imine), N(pyrrole), C(carbanion) and CO. In the crystal structures of **2** and **3**, the equatorial plane consisted of N(imine), N(pyrrole), H(hydride) and CO. The ruthenium centre adopted a distorted-octahedral geometry as reflected in parameters given in Table 1. In the complexes **1**, **2** and **3**, Ru–H bond length (~1.54 Å), CO stretching frequency (ν_{CO}~1920 cm^{-1}) and C–O bond length (~1.15 Å) in addition to Ru–C–O angle (~177°) were consistent with reported values [5a,18].

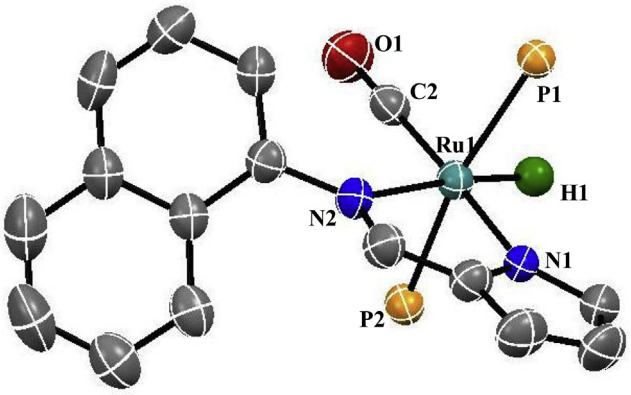

Fig. 2. ORTEP diagram (50% probability level) of the [Ru(L^1N^N)(PPh_3)$_2$(CO)H] (**2**). All hydrogen atoms and PPh_3 groups have been omitted for clarity.

3.4. Catalytic transfer hydrogenation

Role of ruthenium complexes as catalyst in transfer hydrogenation of carbonyl compounds, has gained considerable current attention, most likely due to the relatively mild route of reaction and benign nature of reagents used [5a,b,c,d]. We began our study to utilize complex **1** as a catalyst in transfer hydrogenation of ketones and reaction conditions were optimised using acetophenone as a substrate by varying base, solvent, time and amount of catalyst used. After careful optimisation, we concluded that 0.3 mol% catalyst, 2-propanol as a solvent and 0.3 mmol KOH, provided admirable yield at 85 °C reaction temperature and 6 h of reaction time. Table 2 provides data of various substrates used for transfer hydrogenation. From entries 5 and 6 in Table 2, it is clear that catalyst is completely inactive for substrates 2-pyridyl acetone and 2-amino benzophenone respectively, probably due to the chelate formation of these substrates after coordination to metal centre [5a]. Plausible mechanism for the catalytic transfer hydrogenation of carbonyl compounds using complex **1** is given in Scheme 5 [5a,b,d]. In the first step, deprotonated isopropanol is

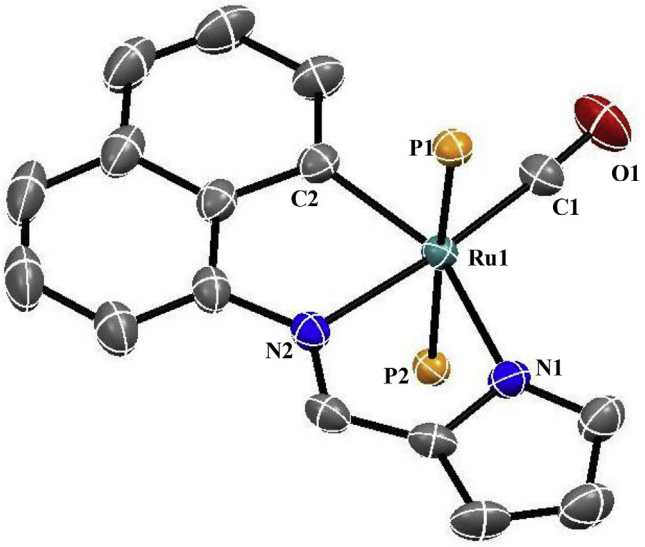

Fig. 1. ORTEP diagram (50% probability level) of the [Ru(L^1C^N^N)(PPh_3)$_2$(CO)] (**1**). All hydrogen atoms and PPh_3 groups have been omitted for clarity.

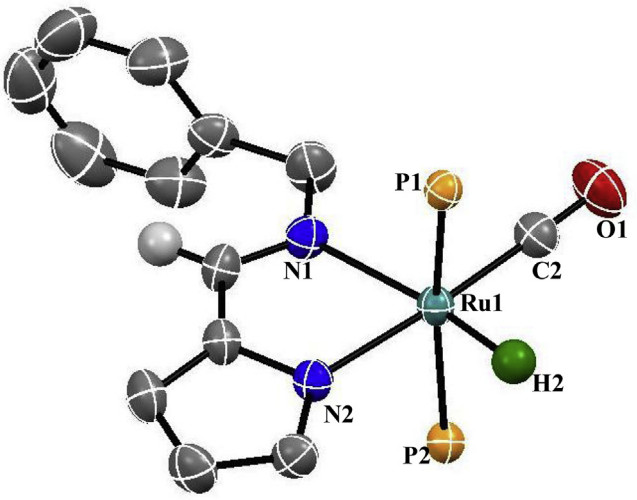

Fig. 3. ORTEP diagram (50% probability level) of the [Ru(L^2N^N)(PPh_3)$_2$(CO)H] (**3**). All hydrogen atoms and PPh_3 groups have been omitted for clarity.

Table 1
Selected bond lengths (Å) and bond angles (deg.) of complexes **1**, **2** and **3**.

Bond lengths (Å) Experimental [Theoretical]		Bond angles (°) Experimental [Theoretical]	
1			
Ru(1)–C(2)	2.070(3) [2.090]	C(1)–Ru(1)–N(1)	110.73(11) [108.91]
Ru(1)–C(1)	1.838(3) [1.856]	N(2)–Ru(1)–N(1)	75.76(9) [76.60]
Ru(1)–N(1)	2.193(2) [2.226]	C(1)–Ru(1)–N(2)	173.44(11) [174.47]
C(1)–O(1)	1.160(4) [1.19]	C(2)–Ru(1)–N(1)	155.28(11) [156.13]
Ru(1)–P(1)	2.387(7) [2.504]	Ru(1)–C(1)–O(1)	176.3(3) [176.27]
Ru(1)–P(2)	2.380(7) [2.505]	P(1)–Ru(1)– P(2)	175.77(2) [176]
Ru(1)–N(2)	2.100(2) [2.122]	C(2)–Ru(1)–N(2)	79.53(10) [79.53]
		C(2)–Ru(1)–C(1)	93.98(12) [94.94]
2			
Ru(1)–H(1)	1.54(2) [1.60]	N(1)–Ru(1)–H(1)	95.5(9) [93.34]
Ru(1)–C(2)	1.839(4) [1.863]	N(2)–Ru(1)–N(1)	75.93(11) [76.49]
Ru(1)–N(1)	2.129(3) [2.134]	H(1)–Ru(1)–N(2)	171.5(9) [169.49]
C(2)–O(1)	1.156(4) [1.193]	C(2)–Ru(1)–N(1)	173.93(13) [174.68]
Ru(1)–P(1)	2.333(10) [2.482]	Ru(1)–C(2)–O(1)	178.5(3) [177.02]
Ru(1)–P(2)	2.373(10) [2.496]	P(1)–Ru(1)– P(2)	164.78(3) [160]
Ru(1)–N(2)	2.225(3) [2.311]	C(2)–Ru(1)–N(2)	98.28(13) [98.20]
		C(2)–Ru(1)–H(1)	90.2(9) [91.94]
3			
Ru(1)–H(2)	1.545 [1.623]	N(1)–Ru(1)–H(2)	93.88 [93.34]
Ru(1)–C(2)	1.843(2) [1.861]	N(2)–Ru(1)–N(1)	76.40(6) [76.45]
Ru(1)–N(1)	2.185(17) [2.227]	H(2)–Ru(1)–N(2)	170.09 [169.78]
C(2)–O(1)	1.149(2) [1.195]	C(2)–Ru(1)–N(1)	100.20(8) [99.43]
Ru(1)–P(1)	2.349(5) [2.476]	Ru(1)–C(2)–O(1)	177.80(19) [177.46]
Ru(1)–P(2)	2.365(5) [2.477]	P(1)–Ru(1)– P(2)	169.02(19) [168.80]
Ru(1)–N(2)	2.122(16) [2.133]	C(2)–Ru(1)–N(2)	176.44(8) [175.84]
		C(2)–Ru(1)–H(2)	89.47 [90.77]

coordinated to ruthenium in catalyst **A** through oxygen atom as isopropoxide and there is simultaneous breaking of Ru–C bond followed by protonolysis of naphthyl ring to generate the intermediate **B**. In the second step, coordinated isopropoxide ligand undergoes β-hydride elimination to generate the Ru–H species in the intermediate **C** which is considered to be catalytically active species during the transfer hydrogenation [5a,b,d]. In the third step, there is insertion of carbonyl substrate into Ru–H bond to generate the intermediate **C**. In the last step, there is elimination of hydrogenated product alcohol with simultaneous regeneration of catalyst.

Table 2
Catalytic transfer hydrogenation of ketones.[a, b]

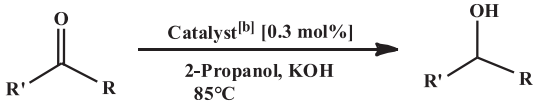

Entry	Substrate	Yield[c] (%)	TON[d]
1		100	333
2		87	290
3		80	266
4		85	283
5		0	0
6		0	0
7		97	323
8		100	333

[a] Reaction conditions: ketone (1.0 mmol), KOH (0.3 mmol), 2-propanol (5 mL), 85 °C.
[b] Catalyst: [Ru(L^1C^N^N)(PPh_3)$_2$(CO)].
[c] Determined by GC–MS.
[d] TON = turnover number.

3.5. DFT studies

The optimisation of geometries for complexes **1**–**3** were performed at the B3LYP level of DFT using LANL2DZ basis set for ruthenium metal. Contour plots of HOMO and LUMO for the all complex **1**–**3** are shown in Fig. 4. Compositions of selected frontier molecular orbitals (HOMO and LUMO) of complexes **1**–**3** are given in Table 3. Moreover, the bond length and bond angle parameters of the optimised structures were compared with data obtained from X-ray calculation in order to validate the experimental data with theoretical (Table 1). The experimental bond length and bond angle values are consistent with theoretical values.

3.6. TDDFT and excited state analysis

To provide insight into the nature of the experimentally derived electronic absorptions, TDDFT calculations were performed on all complexes **1**–**3**. The results of the TDDFT calculations are summarized in Table S2. The bands appearing in the computed absorption spectra were found to be closely related to those of experimental spectra. The TD-DFT spectrum of complex **1** showed transitions at 385 and 477 nm with oscillator strengths (*f*) of 0.0038 and 0.0949 respectively, which were mainly assigned to H → L+3 and H → L transitions respectively. The TD-DFT spectrum of complex **2** showed a transition at 393 nm with oscillator strength (*f*) of 0.0588 which was mainly assigned to H → L+1 transition. Similarly, the TD-DFT spectrum of complex **3** showed a transition at 344 nm, with oscillator strength (*f*) of 0.0168 which was mainly assigned to H → L+1 transition.

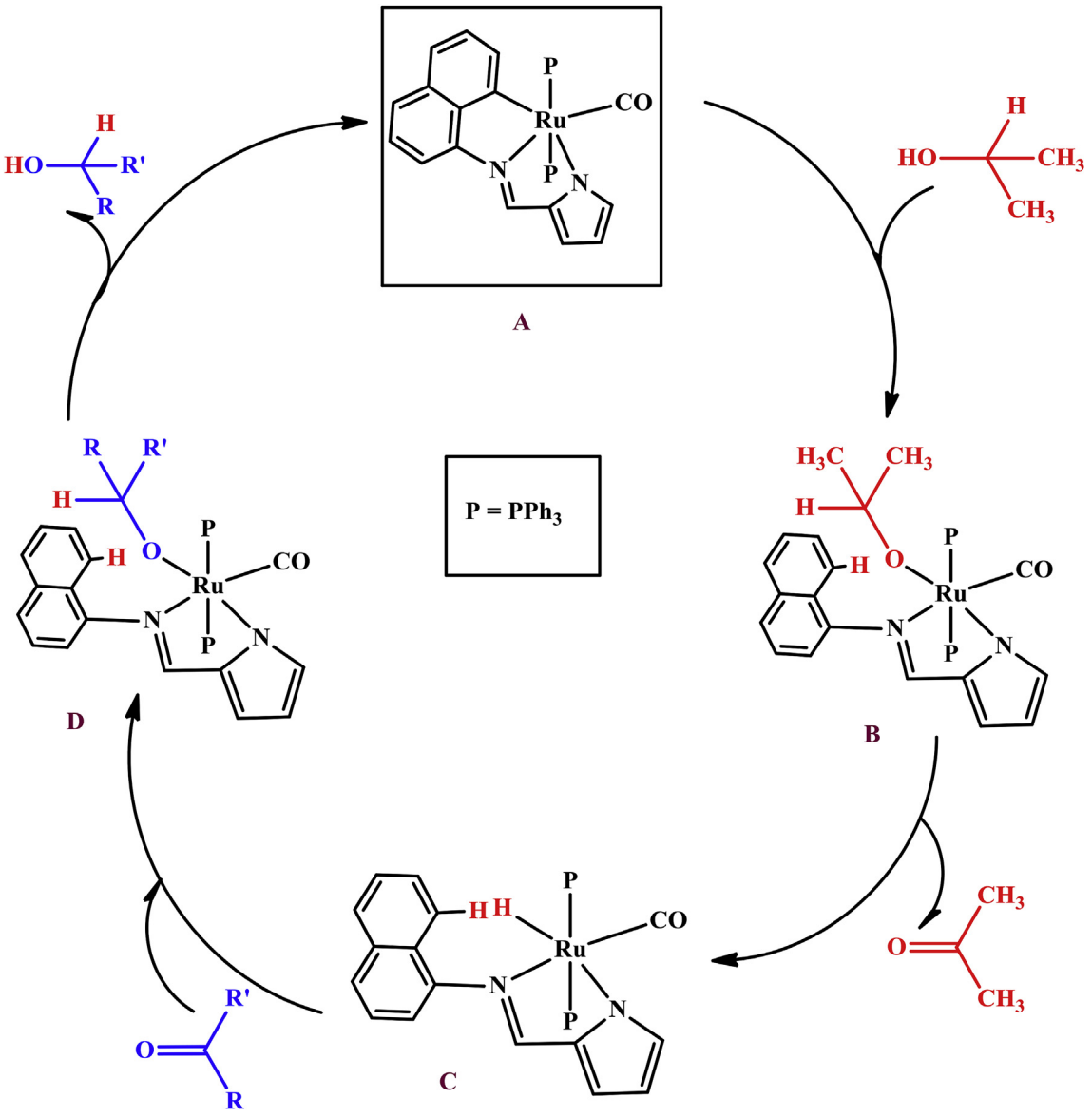

Scheme 5. Plausible mechanism for the catalytic transfer hydrogenation of carbonyl compounds using complex **1**.

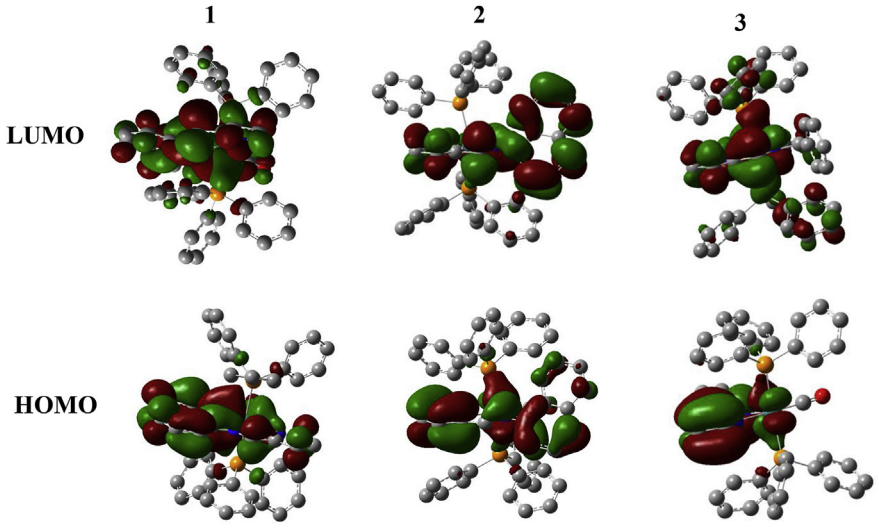

Fig. 4. Contour plots of HOMO and LUMO of complex **1**, **2** and **3**.

Table 3
Compositions of HOMO and LUMO of complexes **1**, **2**, **3**.

Complex	Fragments	Contribution [%] of fragments to	
		HOMO	LUMO
(**1**)	Ru	16	2
	CO	0	2
	PPh_3	5	7
	L^1	79	89
(**2**)	Ru	16	4
	H	0	0
	CO	0	1
	PPh_3	10	10
	L^1H	74	85
(**3**)	Ru	16	17
	H	0	0
	CO	0	3
	PPh_3	12	4
	L^2H	72	76

4. Conclusions

The major findings and conclusions of the present study are following: (**I**) Organometallic ruthenium(II) complex [Ru(L^1C^N^N)(PPh_3)$_2$(CO)] (**1**) was synthesized by reaction of [Ru(PPh_3)$_3$Cl$_2$] with ligand L^1H_2 directly and from complex **2** (intermediate) via C–H bond activation and was characterized by different spectroscopic studies. (**II**) Ruthenium hydrido carbonyl complexes [Ru(L^1N^N)(PPh_3)$_2$(CO)H] (**2**) and [Ru(L^2N^N)(PPh_3)$_2$(CO)H] (**3**) were synthesized by reaction of [Ru(PPh_3)$_3$Cl$_2$] with ligands L^1H_2 and L^2H2, respectively, and characterized by various spectroscopic studies. (**III**) The molecular structures of **1**–**3** were authenticated by X-ray crystallography. (**IV**) Complex **1** was found to be an effective catalyst in transfer hydrogenation reactions of ketones. (**V**) A theoretical study on the structures of the complexes **1**–**3** have been investigated and time-dependent DFT methods were used to aid in the assignment of the intense UV–vis absorption bands found for complexes. (**VI**) The plausible mechanisms for formation of complexes **1**, **2** and catalytic transfer hydrogenation using complex **1** were proposed on the basis of literature.

Acknowledgment

MB is thankful to CSIR, New Delhi for her fellowship. AR and RK are thankful to MHRD (IIT Roorkee) for fellowship. MB, AR, RK are thankful to IIT Roorkee for all facilities. KG is thankful to CSIR, New Delhi (01(2720)/13/EMR-II dated 17-04-2013) for financial assistance.

Appendix A. Supplementary data

Supplementary data to this article can be found online at https://doi.org/10.1016/j.jorganchem.2018.10.034.

References

[1] M. Albrecht, Chem. Rev. 110 (2010) 576–623.
[2] (a) K. Ghosh, S. Kumar, R. Kumar, U.P. Singh, N. Goel, Organometallics 30 (2011) 2498–2505;
(b) K. Ghosh, S. Kumar, R. Kumar, U.P. Singh, Eur. J. Inorg. Chem. (2012) 929–938;
(c) K. Ghosh, S. Kumar, R. Kumar, U.P. Singh, N. Goel, Inorg. Chem. 49 (2010) 7235–7237;
(d) R. Kumar, S. Kumar, M. Bala, A. Ratnam, U.P. Singh, K. Ghosh, RSC Adv. 6 (2016) 72096–72106;
(e) R. Kumar, A. Yadav, A. Ratnam, S. Kumar, M. Bala, D. Sur, S. Narang, U.P. Singh, P.K. Mandal, K. Ghosh, Eur. J. Inorg. Chem. (2017) 5334–5343.
[3] S. Nag, R.J. Butcher, S. Bhattacharya, Eur. J. Inorg. Chem. (2007) 1251–1260.
[4] K. Nagaraju, S. Pal, J. Organomet. Chem. 745–746 (2013) 404–408.
[5] (a) J. Dutta, M.G. Richmond, S. Bhattacharya, Eur. J. Inorg. Chem. (2014) 4600–4610;
(b) H. Chai, T. Liu, Q. Wang, Z. Yu, Organometallics 34 (2015) 5278–5284;
(c) D. Wang, D. Astruc, Chem. Rev. 115 (2015) 6621–6686;
(d) D. Pandiarajan, R. Ramesh, Inorg. Chem. Commun. 14 (2011) 686–689.
[6] M. Kondrashov, D. Provost, O.F. Wendt, Dalton Trans. 45 (2016) 525–531.
[7] M. Ramesh, M.D. Kumar, M. Jaccob, D. Kaleeswaran, G. Venkatachalam, Inorg. Chem. Commun. 85 (2017) 26–31.
[8] H.D. Kasez, R.B. Saillant, Chem. Rev. 72 (1972) 231–281.
[9] K.M. Waldie, A.L. Ostericher, M.H. Reineke, A.F. Sasayama, C.P. Kubiak, ACS Catal. 8 (2018) 1313–1324.
[10] P. Paul, S. Bhattacharya, J. Organomet. Chem. 713 (2012) 72–79.
[11] P. Paul, M.G. Richmond, S. Bhattacharya, J. Organomet. Chem. 751 (2014) 760–768.
[12] T.A. Stephenson, G. Wilkinson, J. Inorg. Nucl. Chem. 28 (1966) 945–956.
[13] G.M. Sheldrick, Acta Crystallogr. A: Found. Crystallogr. 28 (1990) 467–473.
[14] G.M. Sheldrick, SHELXTL – NT 2000 Version 6.12, Reference Manual, University of Gottingen, Pergamon, New York, 1980.
[15] B. Klaus, Diamond, Version 1.2 C, University of Bonn, Germany, 1999.
[16] P. De, S. Maji, A.D. Chowdhury, S.M. Mobin, T.K. Mondal, A. Paretzki, G.K. Lahiri, Dalton Trans. 40 (2011) 12527–12539.
[17] K. Karidi, A. Garoufis, A. Tsipis, N. Hadjiliadis, H. denDulk, J. Reedijk, Dalton Trans. (2005) 1176–1187.
[18] P. Gupta, S. Dutta, F. Basuli, S.M. Peng, G.H. Lee, S. Bhattacharya, Inorg. Chem. 45 (2006) 460–467.